

Terahertz amplifier based on gain switching in a quantum cascade laser

Nathan Jukam^{1*}, Sukhdeep S. Dhillon¹, Dimitri Oustinov¹, Julien Madeo¹, Christophe Manquest², Stefano Barbieri², Carlo Sirtori², Suraj P. Khanna³, Edmund. H. Linfield³, A. Giles Davies³ and Jérôme Tignon¹

Terahertz time-domain spectroscopy is widely used in a broad range of applications where knowledge of both the amplitude and phase of a terahertz wave can reveal useful information about a sample¹. However, a means of amplifying terahertz pulses, which would be of great benefit in improving the applicability of time-domain spectroscopy, is lacking. Although terahertz quantum cascade lasers² are promising devices for terahertz amplification³, gain clamping⁴ limits the attainable amplification⁵. Here, we circumvent gain clamping and demonstrate amplification of terahertz pulses by ultrafast gain switching of a quantum cascade laser through the use of an integrated Auston switch⁶. This unclamps the gain by placing the laser in a non-equilibrium state that allows large amplification of the electromagnetic field within the cavity. This technique offers the potential to produce high field terahertz pulses that approach the quantum cascade laser saturation field.

Terahertz time-domain spectroscopy (TDS) is a powerful technique used to generate and detect pulses of broadband terahertz radiation¹. It is now widely used in terahertz imaging⁷, non-destructive testing⁸ and complex compound detection⁹. To generate terahertz pulses, near-infrared femtosecond lasers are used to excite photoconductive antennas¹⁰ or nonlinear crystals¹¹. Although the peak terahertz electric fields generated by these sources can be relatively high, the field amplitude per unit frequency is rather small owing to the extremely large spectral bandwidth of the generated terahertz pulse. Larger terahertz field amplitudes can be realized by increasing the power of the femtosecond laser. However, this requires large, complex and costly regenerative Ti:sapphire amplifier systems¹¹. A compact, practical and direct amplifier of terahertz pulses would therefore be of great interest.

A promising candidate for a terahertz amplifier is the recently realized terahertz quantum cascade laser (QCL)². In this semiconductor-based source, laser action takes place through electronic inter-sub-band transitions¹². Recently terahertz TDS has been used to measure the gain spectra of QCLs³. In these experiments, the QCL essentially acts as an amplifier of terahertz probe pulses transmitted through the laser¹³. However, the amplification is limited by gain clamping, which fixes the gain to the sum of the waveguide and mirror losses during laser action. Amplification can be increased by reducing the mirror reflectivity through the use of anti-reflection coatings³. However, even for relatively high terahertz frequencies, low-loss dielectric anti-reflection coatings are extremely challenging to realize¹⁴ owing to the large coating thicknesses required. Tapered QCLs can also be used to amplify terahertz radiation¹⁵. However, the flared facets of tapered amplifiers are extremely wide and their output suffers from severe

astigmatism¹⁶. This precludes their use in TDS, in which high beam quality and a tight focus on the detector are essential to maximize the measured field.

Here, we use the technique of gain switching^{17–19}, which consists of turning on the gain of a laser on a timescale that is much faster than the build-up time of the laser field. During this period, the gain is greater than the total losses and unclamped from its value at threshold. The bare cavity gain of the laser (that is, the unclamped gain in the absence of a laser field) can therefore be accessed, and used to amplify injected terahertz probe pulses. In this paper, we demonstrate large terahertz pulse amplification (up to 26 dB excluding coupling losses) that is well above the limits imposed by the mirror losses and gain clamping. The gain switching is performed by an Auston switch⁶ integrated into the QCL, where femtosecond illumination allows photo-excited carriers to change the resistance of the switch from an insulating to a conductive state on an ultrafast timescale.

The active region of the QCL used in our work is based on a bound-to-continuum design²⁰, which has been modified to lase at 2.4 THz. A schematic of the device is shown in Fig. 1a. Electrons from the top of the QCL ridge flow down through the active region to a highly doped n⁺⁺ layer. From the n⁺⁺ layer, electrons flow horizontally to two annealed AuGeNi contact layers on each side of the ridge. The integrated Auston switch was realized by etching an 80- μm gap through one of the AuGeNi contact layers down to the semi-insulating GaAs substrate. Processed samples were cleaved into laser bars of 1.5 mm in length.

An electrical schematic of the sample is given in Fig. 1b. The QCL can be represented as a capacitor in parallel with a shunt resistor. The lower n⁺⁺ layer can be treated as a resistance in series with the QCL, and the Auston switch as a capacitor that shorts when illuminated by a femtosecond laser. The QCL and Auston switch are independently biased by two external circuits that share a common ground. This permits the QCL to be biased just below threshold, which significantly reduces the current needed from the Auston switch to drive the laser above threshold. The Auston switch, QCL ridge and the common ground are connected to external circuits with bond wires. When the femtosecond laser illuminates the Auston switch (ON state) the voltage of the common ground changes on an ultrafast (picosecond) timescale. This drives an electrical pulse through an RC circuit formed by the resistive n⁺⁺ layer and the capacitance of the QCL. At longer timescales the external circuit will restore the voltages on the device to their original values. Without femtosecond laser illumination the Auston switch is highly resistive and hence in the OFF state.

Figure 1c shows the characteristic light–current density (L – J) and voltage–current density (V – J) curves of the device at 7 K without

¹Laboratoire Pierre Aigrain, École Normale Supérieure, UMR 8551 CNRS, UPMC Université Paris 6 75005 Paris, France, ²Matériaux et Phénomènes Quantiques, Université Denis Diderot—Paris 7, UMR 7162 CNRS, 75013 Paris, France, ³School of Electronic and Electrical Engineering, University of Leeds, Leeds LS2 9JT, UK. *e-mail: nathan.jukam@lpa.ens.fr

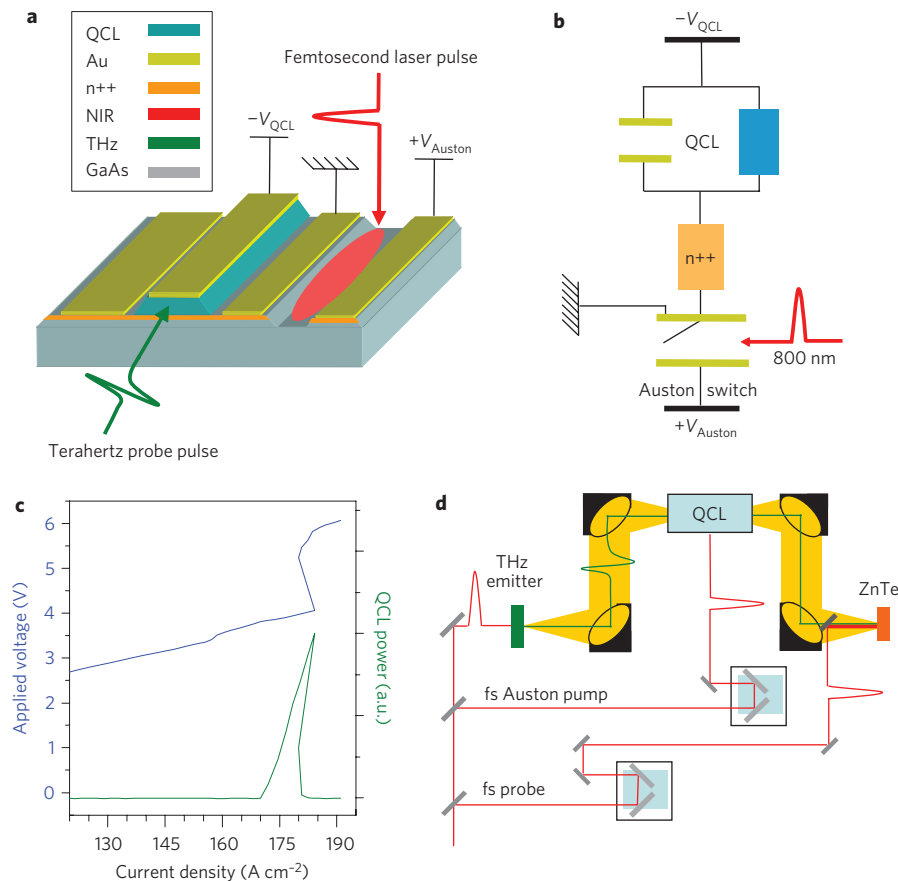


Figure 1 | Terahertz QCL with an integrated Auston switch. **a**, Schematic of the QCL with an Auston switch integrated into one of the side contacts. **b**, Electrical diagram of the QCL and Auston switch. The QCL is represented as a capacitor and a resistor in parallel. The Auston switch and QCL share a common ground and can be biased independently. **c**, Pulsed light-current and voltage-current curves of the 2.4 THz QCL at 7 K. The threshold current density is 172 A cm^{-2} and maximum power occurs at 184 A cm^{-2} . **d**, Schematic of the experimental apparatus.

illumination of the Auston switch. The laser threshold is 172 A cm^{-2} , and maximum power occurs at 184 A cm^{-2} . The negative differential resistance in the V - J curve corresponds to a drop in output power, owing to misalignment of the bandstructure²⁰.

Figure 1d shows a schematic of the experimental arrangement. Broadband terahertz probe pulses are generated by discharging a photoconductive antenna with the same femtosecond laser that is used to excite the Auston switch. The terahertz probe pulses are then coupled into the QCL waveguide through the end facets. The transmitted pulses are measured using free-space electro-optic sampling (which is insensitive to the QCL laser emission⁴) in conjunction with a delay line for the femtosecond detection beam. Using a reference pulse, amplification of the terahertz probe pulse and the gain of the terahertz QCL can be determined¹³. Another delay line, for the femtosecond laser beam that activates the Auston switch, permits the time delay between the Auston switch and the terahertz probe pulse to be varied. (Further details can be found in the Methods.)

Owing to facet reflectivity, when the injected terahertz probe pulse reaches the output facet, part of the pulse is transmitted (single pass) and the remaining part is reflected back into the QCL cavity. The reflected pulse undergoes a series of multiple passes through the cavity, and hence has a longer amplification length. Figure 2a–d shows the electric fields of the terahertz probe pulses transmitted through the QCL for 1, 3, 5 and 7 passes with the Auston switch ON (blue lines) and OFF (black lines). The corresponding spectra of the fields are shown in Fig. 2e–h. For each scan the time delay between the Auston switch and the terahertz

probe pulse was adjusted to maximize the output pulse. The QCL is biased just below laser threshold, at a current density of 168 A cm^{-2} , in order to minimize the current that needs to be injected by the Auston switch.

For the single pass, with the Auston switch ON, we observe an increase in the number of field oscillations (Fig. 2a) and a larger spectral amplitude (Fig. 2e) compared to the Auston switch OFF. Figure 2b,c shows the electric fields of output pulses that undergo multiple passes in the QCL (3 and 5 passes, respectively). With the Auston switch OFF, the amplitude of the transmitted pulse decreases as the number of passes through the QCL increases, as expected²¹. However, with the Auston switch ON, the field amplitude increases considerably as the terahertz probe pulses undergo more passes through the QCL. This indicates clearly that the gain of the cavity is greater than the total losses, and no longer clamped. In Fig. 2g, the pulse power amplification at 2.46 THz is 26 dB after five passes through the QCL compared to the value with the Auston switch OFF. Figure 2d (red curve) shows the field of a probe pulse after seven passes with the Auston switch OFF, and the current density above threshold (178 A cm^{-2}). This shows that the large amplification with the Auston switch ON in Fig. 2d (blue curve) arises from unclamping the gain by an ultrafast turn-on of the device, and not merely by increasing the current above threshold.

Figure 2c,d shows that the amplification of the probe pulses eventually saturates as the number of passes through the QCL continues to increase. This occurs because the electrical pulse produced by the Auston switch (and hence the unclamped gain) has a finite time

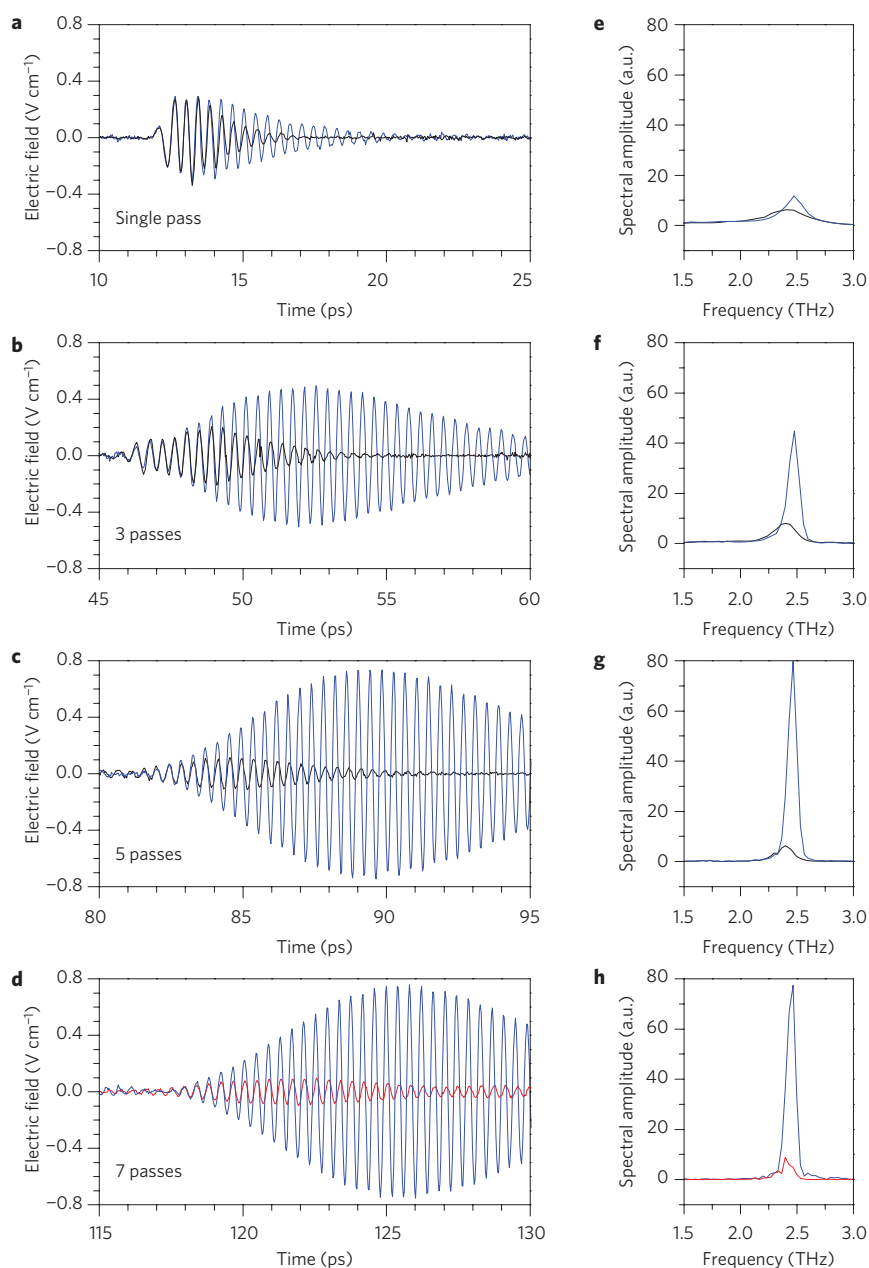


Figure 2 | Fields and spectra of the terahertz probe pulses with the Austin switch ON and OFF. The QCL is biased just below threshold at a current density of 168 A cm^{-2} . A voltage of 27.5 V is applied to the Austin switch. **a-h**, The blue (black) curves show the difference electric field (**a-d**) and spectra (**e-h**) with (without) femtosecond laser illumination on the Austin switch. The red curves in **d** and **h** show the difference electric field and spectra without femtosecond illumination of the Austin switch for a current above threshold at 178 A cm^{-2} . The difference electric field of the terahertz probe pulses transmitted through the QCL for a single pass (**a**), 3 (**b**), 5 (**c**) and 7 (**d**) passes, respectively, with **e-h** showing the corresponding spectra of the fields.

duration. Pulse amplification ceases once the electrical pulse ends, and the gain eventually returns to its clamped value. The finite duration of the electrical pulse can be inferred from Fig. 3, where the single-pass gain is plotted as a function of the time delay between the terahertz probe pulse and the femtosecond pulse that activates the Austin switch. The gain increases for 60 ps, after which it decreases and the net amplification of the probe pulse eventually declines. Each point in Fig. 3 is a measure of the instantaneous gain convolved with the 18 ps single-pass transit time of the probe pulse. The duration of the excess gain and hence the electrical pulse is in the order of 100 ps.

The gain does not switch on instantaneously, and the rise time of the gain is found to be ~ 46 ps (in the range 10–90%) from Fig. 3a. This is in rough agreement with a calculated rise time of 26 ps,

which is derived from the RC time constant of the calculated n^{++} resistance (3.2Ω) and the capacitance of the QCL (3.7 pF). The rise time could be significantly reduced by using a metal-metal waveguide²², which would replace the resistive n^{++} layer under the QCL active region with a metal layer. From Fig. 3 it can also be observed that for very long periods (>140 ps) the gain decreases below its value at negative times. This is caused by an LC resonance and a corresponding voltage oscillation, in which the external circuit recharges the common ground of the Austin switch and QCL (see Supplementary Information for further details).

The gain as a function of the current density with the Austin switch ON (corresponding to 60 ps in Fig. 3) and with the Austin switch OFF (corresponding to -140 ps) is shown in Fig. 4a. (The current density in Fig. 4 is the ‘continuous-wave’

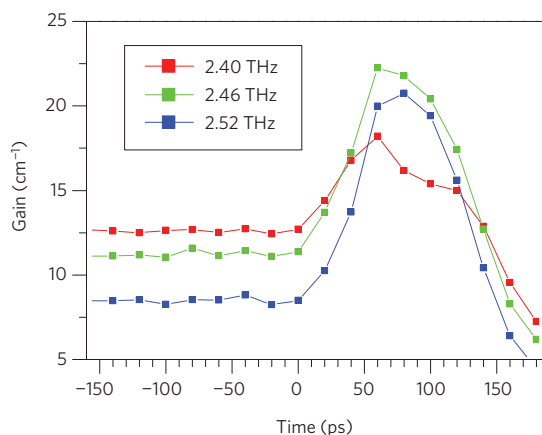


Figure 3 | Duration of the unclamped gain created by the Auston switch. Single-pass gain at 2.40 THz (red), 2.46 THz (green) and 2.53 THz (blue) plotted as a function of the time delay between the terahertz probe pulse and the femtosecond laser pulse that turns on the Auston switch. The QCL is biased at a current density of 168 A cm^{-2} and the voltage applied to the Auston switch is 27.5 V. (Positive time delays correspond to the Auston switch pulse arriving before the terahertz probe pulse.).

current density and excludes the current generated by the Auston switch.) With the Auston switch OFF, the gain clamps as expected after threshold (172 A cm^{-2}) at a value of 12.5 cm^{-1} . With the Auston switch ON the gain is $\sim 10 \text{ cm}^{-1}$ greater than the clamped gain, which gives rise to the large amplification observed in Fig. 2 for the multiple-pass pulses. This shows that the transmitted pulses are amplified at the bare cavity gain (that is, the gain in the absence of the laser field) with the Auston switch ON. The generated ultrafast electrical pulse essentially increases the voltage and current across the QCL before the laser field can build up, increasing the gain without being limited to the clamped value. Indeed, an estimate of the current provided by the Auston switch can be found by comparing the current densities for which the centre gain is identical for the Auston switch being ON and OFF ($\sim 35 \text{ A cm}^{-2}$; Fig. 4b). For current densities above threshold, there is a significant internal laser field inside the laser cavity that saturates the bare cavity gain, and reduces the gain to its clamped value at threshold. Thus the excess gain between the bare cavity and clamped gain cannot be used for pulse amplification. This explains the drop in the gain after threshold with the Auston switch ON. (There could also be a contribution from the electric pulse driving the QCL to current densities beyond the maximum power and towards the shut-off current.) Note that this technique also allows the measurement of the maximum bare cavity gain of terahertz QCLs (22.4 cm^{-1} for the current device).

Figure 4b shows the increase in the centre frequency of the gain as a function of current density. With the Auston switch ON (red curve), the centre frequency is shifted to higher frequencies than when the Auston switch is OFF (black curve). This frequency shift is most likely the result of a small Stark shift of the upper laser levels caused by the QCL being driven to higher biases by the Auston switch. The shift in frequency can also be observed in Fig. 3 where, before the Auston switch is switched ON, the gain is highest at 2.40 THz, whereas the maximum of the unclamped gain peaks at 2.46 THz (at 60 ps).

Increases in the value of the amplified fields could be obtained by using QCLs with a greater bare cavity gain (for example, longitudinal optical phonon based QCLs, by improving the coupling efficiency of the terahertz pulse into the QCL (currently only of the order of a few percent), and by increasing the length of the QCL cavity (which would reduce losses from the QCL facets). More

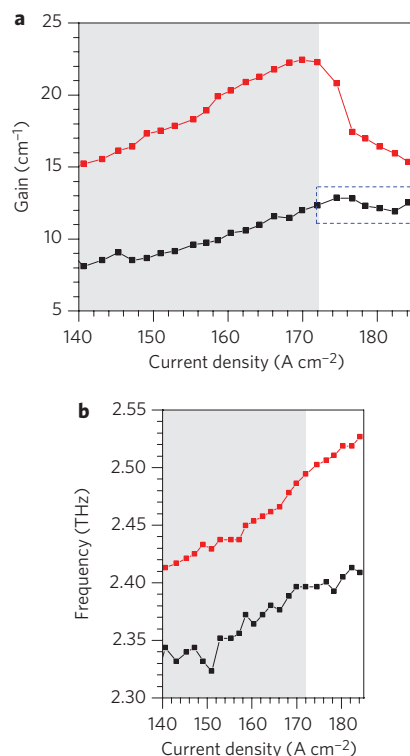


Figure 4 | Gain with the Auston switch OFF and ON—clamped and unclamped gain. **a**, The single-pass gain as a function of current density for two different time delays. The red line shows the gain with the Auston switch ON (corresponding to 60 ps in Fig. 3). The black line shows the gain with the Auston switch OFF (corresponding to -140 ps in Fig. 3). The blue dashed box corresponds to the clamped gain. **b**, The centre frequency of the gain as a function of current density with the Auston switch turned ON (red) and the Auston switch turned OFF (black). The grey shading indicates current densities below threshold. To increase the frequency resolution the data was zero padded.

importantly, the amplification is only limited by the finite duration of the electrical pulses generated by the Auston switch. By increasing their duration by device engineering (see Supplementary Information), terahertz probe pulses could potentially be amplified until their fields approach the internal saturation fields of terahertz QCLs (up to $\sim 1 \text{ kV cm}^{-1}$). This would effectively injection-lock the QCL to the terahertz probe pulses, and provide a high field source of terahertz radiation. This could then be used to generate high-field narrowband terahertz pulses^{23,24}, which would be of considerable interest in the study of single transitions, nonlinear phenomena and coherent effects in the terahertz frequency range^{25,26}. Equally, it could be applied to generate high fields over a broad spectral range, using multiple QCL active regions to give a larger gain width²⁷.

In conclusion, picosecond gain switching of a terahertz QCL has been demonstrated using an integrated Auston switch. The ultrafast switching placed the laser in a transient state in which the gain was no longer clamped, and so could exceed the total losses of the cavity. Consequently, the QCL bare cavity gain was used to produce large amplification of terahertz pulses from a TDS system. These results show that gain-switched QCL amplifiers of terahertz pulses could significantly advance the current state of terahertz technology and extend the applications of terahertz TDS and QCLs.

Methods

The terahertz probe pulses were generated by illuminating an inter-digitated photoconductive antenna with 360 mW of average power from a 76 MHz

femtosecond source (pulsewidth, 80 fs; centre wavelength, 820 nm). The interdigitated GaAs antenna had a gap spacing of 1.5 μm and a bias of 4 V was applied. The 0.5-mm-thick antenna was bonded to a 1-mm high-resistivity silicon wafer, which extended the time between echoes caused by internal reflections. The free-space terahertz radiation was collected and refocused onto the sample (and subsequently the electro-optic crystal for detection) with f#2 parabolic mirrors. Measurements were taken at 7 K in a helium flow cryostat. A small 200- μm -diameter hole in a metal shim was placed in front of the entrance facet of the QCL. A 500 μm <110> ZnTe crystal was used for electro-optic detection of the transmitted terahertz pulses. A 2-mm <100> ZnTe wafer (which has a null electro-optic effect) was attached to the back side of the <110> ZnTe crystal to extend the time delay of the echoes.

The antenna was modulated at 50 kHz with a duty cycle of 50%. The QCL was modulated at 25 kHz with a 25% duty cycle, such that every other QCL pulse was coincident with an antenna pulse. By locking into the modulation frequency of the QCL, the difference between the terahertz electric field with the QCL on and off was measured (the difference field).

The active region of the QCL consisted of 90 periods of **1.8 / 12.4 / 1.5 / 15.3 / 0.6 / 10.0 / 0.6 / 13.5 / 4.2 / 11.8 / 3.5 / 11.3 / 2.7 / 11.4 / 2.0 / 12.0 / 2.0 / 118.0** layers of GaAs ($\text{Al}_{0.15}\text{Ga}_{0.85}\text{As}$ barriers in bold). The 11.4-nm and 12.0-nm GaAs layers were nominally doped at $1.6 \times 10^{-16} \text{ cm}^{-3}$. The QCL was grown on an undoped GaAs substrate, and the active region was sandwiched between an 80-nm top contact layer and a 700-nm bottom n^{++} contact layer. A 300-nm $\text{Al}_{0.5}\text{Ga}_{0.5}\text{As}$ barrier layer separated the lower n -GaAs layer from the undoped GaAs substrate.

Devices were processed into a single plasmon geometry with a ridge width of 250 μm , and the QCLs were mounted onto a gold-coated copper mount to improve heat dissipation.

The voltage applied to the Auston switch (27.5 V) was chosen to maximize the output fields of the terahertz probe pulses. The large Auston switch voltage is most likely due to the large ratio of the QCL capacitance (3.7 pF) to the Auston switch capacitance (0.16 pF) and the 300-nm-thick $\text{Al}_{0.5}\text{Ga}_{0.5}\text{As}$ etch stop layer between the bottom n^{++} layer and the substrate.

A d.c. voltage was applied across the Auston switch to reduce electrical noise pick-up. The Auston switch was excited with an average power of 390 mW by the femtosecond laser. A 200-mm achromatic lens focused the beam onto the Auston switch, and a 50-mm divergent cylindrical lens was used to expand the beam along the length of the QCL. The resulting beam profile was roughly matched to the area of the Auston switch. A webcam-based imaging system verified that the laser spot overlapped with the Auston switch.

Received 6 July 2009; accepted 19 October 2009;
published online 22 November 2009

References

1. Tonouchi, M. Cutting edge terahertz technology. *Nature Photon.* **1**, 97–105 (2007).
2. Köhler, R. *et al.* Terahertz semiconductor-heterostructure laser. *Nature* **417**, 156–159 (2002).
3. Kroll, J. *et al.* Phase resolved stimulated emission measurements in a laser. *Nature* **449**, 698–700 (2007).
4. Jukam, N. *et al.* Investigation of spectral gain narrowing in quantum cascade lasers using terahertz time domain spectroscopy. *Appl. Phys. Lett.* **93**, 101115 (2008).
5. Koestor, C. J. & Snitzer, E. Amplification in a fiber laser. *Appl. Opt.* **3**, 1182–1186 (1964).
6. Auston, D. H. Picosecond optoelectronic switching and gating in silicon. *Appl. Phys. Lett.* **26**, 101–103 (1975).
7. Chan, W. L., Deibel, J. & Mittleman, D. M. Imaging with terahertz radiation. *Rep. Prog. Phys.* **70**, 1325–1379 (2007).
8. Stoik, C. D., Bohm, M. J. & Blackshire, J. L. Nondestructive evaluation of aircraft composites using transmissive terahertz time domain spectroscopy. *Opt. Express* **16**, 17039–17051 (2008).
9. Shen, Y. C. *et al.* Detection and identification of explosives using terahertz pulse spectroscopic imaging. *Appl. Phys. Lett.* **86**, 241116 (2005).
10. Dreyhaupt, A., Winnerl, S., Dekorsy, T. & Helm, M. High intensity terahertz radiation from a microstructure large-area photoconductor. *Appl. Phys. Lett.* **86**, 121114 (2005).

11. Löffler, T., Hahn, T., Thomson, M., Jacob, F. & Roskos, H. G. Large-area electro-optic ZnTe terahertz emitters. *Opt. Express* **13**, 5355–5362 (2005).
12. Williams, B. S. Terahertz quantum cascade lasers. *Nature Photon.* **1**, 517–525 (2007).
13. Jukam, N. *et al.* Gain measurements of quantum cascade lasers using terahertz time domain spectroscopy. *IEEE J. Sel. Top. Quantum Electron.* **14**, 436–442 (2008).
14. Xu, J. *et al.* Tunable terahertz quantum cascade lasers with an external cavity. *Appl. Phys. Lett.* **91**, 121104 (2007).
15. Mauro, C. Amplification of terahertz radiation in quantum cascade structures. *J. Appl. Phys.* **102**, 063101 (2007).
16. Walpole, J. N. Semiconductor amplifiers and lasers with tapered gain regions. *Opt. Quantum Electron.* **28**, 623–645 (1996).
17. Duguay, M. A. & Damen, T. C. Picosecond measurement of spontaneous and stimulated emission from injection lasers. *Appl. Phys. Lett.* **40**, 667–669 (1982).
18. Göbel, O. *et al.* Direct gain modulation of a semiconductor laser by a GaAs picosecond optoelectronic switch. *Appl. Phys. Lett.* **42**, 25–27 (1983).
19. Paiella, R. *et al.* High-speed operation of gain-switched midinfrared quantum cascade lasers. *Appl. Phys. Lett.* **75**, 2536–2538 (1999).
20. Barbieri, S. 2.9 THz quantum cascade lasers operating up to 70 K in continuous wave. *Appl. Phys. Lett.* **85**, 1674–1676 (2004).
21. Parz, W. Ultra fast probing of light matter interaction in a midinfrared quantum cascade laser. *Appl. Phys. Lett.* **93**, 091105 (2008).
22. Dhillon, S. *et al.* Ultralow threshold current terahertz quantum cascade lasers based on double-metal buried strip waveguides. *Appl. Phys. Lett.* **87**, 071107 (2005).
23. Lee, Y. S., Meade, T., Perlin, V., Winful, H. & Norris, T. B. Generation of narrow-band terahertz radiation via optical rectification of femtosecond pulses in periodically poled lithium niobate. *Appl. Phys. Lett.* **76**, 2505–2507 (2000).
24. Danielson, J. R. *et al.* Intense band terahertz generation via type II difference-frequency generation in ZnTe using chirped optical pulses. *J. Appl. Phys.* **104**, 033111 (2008).
25. Cole, B. E., Williams, J. B., King, B. T., Sherwin, M. S. & Stanley, C. R. Coherent manipulation of semiconductor quantum bits with terahertz radiation. *Nature* **410**, 60–63 (2001).
26. Carter, S. G. Quantum coherence in an optical modulator. *Science* **310**, 651–653 (2005).
27. Freeman, J. R., Marshall, O. P., Beere, H. E. & Ritchie, D. A. Electrically switchable emission in terahertz quantum cascade lasers. *Opt. Express* **16**, 19830–19834 (2008).

Acknowledgements

This work was financially supported by the Direction Générale de l'Armement (DGA), Centre de compétence NanoSciences (CNano), Agence Nationale de la Recherche (ANR), Engineering and Physical Sciences Research Council (EPSRC) and the EC NOTES programme. The Laboratoire Pierre Aigrain, École Normale Supérieure (LPA-ENS) is a 'Unité Mixte de Recherche Associée au Centre Nationale de la Recherche Scientifique (CNRS) UMR8551 et aux Universités Paris 6 et 7'. Device fabrication was performed at the nanocentre Institut d'Électronique Fondamentale-Minerve (CTU-IEF-Minerve), which was partly funded by the 'Conseil General de l'Essonne'.

Author contributions

Data were taken by N.J., S.S.D., D.O. and J.M., and analysed by N.J. and S.S.D. The experiment was conceived by N.J. Samples were grown by S.P.K., E.H.L. and A.G.D., and processed by C.M., S.B. and C.S. The manuscript was prepared by N.J., S.S.D. and J.T. with contributions from S.B., C.S. and E.H.L. J.T. and S.S.D. supervised and coordinated all work.

Additional information

Supplementary information accompanies this paper at www.nature.com/naturephotonics. Reprints and permission information is available online at <http://npg.nature.com/reprintsandpermissions/>. Correspondence and requests for materials should be addressed to N.J.